Quasi-one-dimensional molecular magnets based on derivatives of (fluorobenzyl)pyridinium with the [M(mnt)$_2$] monoanion (M = Ni, Pd or Pt; mnt^{2-} = maleonitriledithiolate): Syntheses, crystal structures and magnetic properties†

X. M. Ren,*[a,g] S. Nishihara,[b] T. Akutagawa,[a,g] S. Noro,[a,g] T. Nakamura,*[a,g] W. Fujita,[c] K. Awaga,[d] Z. P. Ni,[e] J. L. Xie,[e] Q. J. Meng[e] and R. K. Kremer[f]

Received 7th October 2005, Accepted 5th January 2006
First published as an Advance Article on the web 23rd January 2006
DOI: 10.1039/b514278d

The syntheses, structural characterizations and magnetic behaviors of three new complexes, 1-(3′,4′,5′-trifluorobenzyl)pyridinium [M(mnt)$_2$]$^-$ [M = Ni (**1**), Pd (**2**) or Pt (**3**)], are reported. These complexes are isomorphous and their prominent structural character is that the [M(mnt)$_2$]$^-$ anions form columnar stacks, in which the dimerization was observed. Complexes **2** and **3** are diamagnetic, while **1** possesses an energy gap of 2474 K. For crystal **4**, 1-(4′-fluorobenzyl)pyridinium [Ni(mnt)$_2$] (its structure and magnetic susceptibility were briefly reported earlier), the magnetic behavior can be divided into two regimes, namely, weakly ferromagnetic coupling above 93 K and strongly antiferromagnetic coupling below 93 K. A transition occurs at 93 K which switches the magnetic exchange nature from ferromagnetic to antiferromagnetic. A sharp thermal abnormality with λ-shape, associated with the transition, appears from its heat capacity measurement to indicate that the transition is first order. The temperature dependences of the superlattice diffractions revealed the existence of the pretransitional phenomena up to at least 140 K. The unusual magnetic behavior of **4**, such as the origin of the ferromagnetic interaction in the high temperature phase and what causes the spin transition, are discussed further.

Introduction

Solids consisting of molecules with flat-shaped configurations and extended electronic structures have been attracting considerable interest in the field of molecule-based conductors and magnets due to their unusual physical properties.[1–4]

Our studies have been focused on the design, preparation, and investigation of novel spin transition molecular magnets that are based on the molecular architecture of [M(mnt)$_2$]$^-$ (mnt^{2-} = maleonitriledithiolate; M = Ni, Pd, or Pt). The formation of columnar stacks is favored because such molecules possess (1) a flat molecular and extended electronic structure, and (2) intermolecular interactions between [M(mnt)$_2$]$^-$ anions, such as π–π stacking, S···S or S···M interactions. The magnetic exchange characteristic is highly sensitive to the intermolecular contacts and overlap pattern between neighboring anions within an anionic stack,[4c,5] so that an external perturbation could trigger a spin transition. Accordingly, a key issue in our research is the control of the [M(mnt)$_2$]$^-$ anions during the columnar arrangement. Because the stacking pattern of the [M(mnt)$_2$]$^-$ anion depends strongly upon the molecular topology of the countercation, we proposed that the formation of a columnar stack of [M(mnt)$_2$]$^-$ was attainable by modifying the molecular structure of the countercation. Derivatives of benzylpyridinium (abbreviated as [RBzPy]$^+$) can serve as flexible cations which can be adjusted *via* modifying the nature of the groups on the aromatic rings.[6] Consequently, we have recently prepared a series of [RBzPy][M(mnt)$_2$] ion-pair complexes that form a structure with segregated stacks of cation and anion,[7,8] and in some of these a spin-Peierls-like transition was observed (the substituent groups in the cation and the metal ions of the anion for those reported complexes are listed in Table 1).[8]

Recently, we briefly reported the room temperature crystal structure of and the temperature dependence of the magnetic susceptibility for [1-(4′-fluorobenzyl)pyridinium][Ni(mnt)$_2$] (the [FBzPy][Ni(mnt)$_2$] complex is referred to in the current work as compound **4**), which undergoes a spin transition at ~93 K.[8k] The nature of the magnetic exchange is weakly ferromagnetic above this transition (high temperature phase) and strongly

---

[a] *Research Institute for Electronic Science, Hokkaido University, Sapporo, 060-0812, Japan. E-mail: xmren@es.hokudai.ac.jp, tnaka@imd.es.hokudai.ac.jp; Fax: +81 11-706-4972; Tel: +81 11-706-2849*
[b] *Department of Physical Science, Graduate School of Science, Osaka Prefecture University, Sakai, Osaka, 599-8531, Japan*
[c] *Research Center of Materials Science, Nagoya University, Chikusa-ku, Nagoya, 464-8602, Japan*
[d] *Department of Chemistry, Graduate School of Science, Nagoya University, Chikusa-ku, Nagoya, 464-8602, Japan*
[e] *State Key Laboratory & Coordination Chemistry Institute, Nanjing University, 210093, Nanjing, P. R. China*
[f] *Max-Planck-Institut für Festkörperforschung, Heisenbergstrasse 1, Postfach 800665, D-70569, Stuttgart, Germany*
[g] *CREST, Japan Science and Technology Corporation (JST), Kawaguchi, 332-0012, Japan*

† Electronic supplementary information (ESI) available: Bond lengths for the anion in compounds **1–4** (Table S1); spin density distributions in a monomer of [Ni(mnt)$_2$]$^-$ (Table S2); details of DFT calculations; ORTEP and stacking pattern diagrams for **2–4** (Fig. S1–S5); and the EPR spectrum of **4** (Fig. S6). See DOI: 10.1039/b514278d

Table 1 Reported complexes in the series of $[R^1R^2R^3BzPy][M(mnt)_2]$ that exhibit a magnetic transition

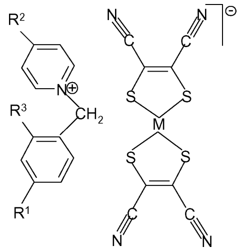

R_1	R_2	R_3	M	Reference
I	H	H	Ni	[8*a*]
NO_2, Cl, Br	H	H	Ni	[8*i*]
F	H	H	Ni	[8*k*]
CN	H	H	Ni	[8*h*]
NO_2, Cl, Br	H	H	Pt	[8*e*]
Br	H	F	Ni	[8*f*]
Br	NH_2	H	Ni	[8*g*]
CN	NH_2	H	Ni	[8*c*]
Cl, H	NH_2	H	Ni	[8*b*,8*j*]
Vinyl	H	H	Ni	[8*d*]

antiferromagnetic below (low temperature phase). This magnetic behavior is significantly different from other spin transition complexes of $[RBzPy][Ni(mnt)_2]$ in which the natures of the magnetic exchange are weakly and strongly antiferromagnetic in the high and low temperature phases, respectively. It appears that a delicate relationship exists between the nature of substituent group (such as its electronic or steric nature) and the anionic stacking pattern, as well as the magnetic coupling behavior in the series $[RBzPy][M(mnt)_2]$ (M = Ni, Pd or Pt).[7–9] In this work, a new countercation, 1-(3′,4′,5′-trifluorobenzyl)pyridinium (abbreviated as $[F_3BzPy]^+$) together with three new complexes, $[F_3BzPy][M(mnt)_2]$ (M = Ni, Pd or Pt), were designed and prepared to gain more insight into the issues mentioned above and to investigate the magnetostructural relationship. The crystal structures and magnetic properties for these new complexes were examined. Additionally, the nature of the magnetic transition in $[FBzPy][Ni(mnt)_2]$ was further investigated by heat capacity as well as temperature dependent superlattice diffraction measurements.

Experimental

Preparation of the complexes

Na_2mnt, the derivatives of fluoro-substituted benzylpyridinium bromide[6] and their salts with the $[M(mnt)_2]$ dianion (M = Ni, Pd or Pt) were prepared according to the published procedures.[10]

$[F_3BzPy][Ni(mnt)_2]$ (1)

To a solution of $[F_3BzPy]_2[Ni(mnt)_2]$ (844 mg, 1.0 mmol) in acetonitrile (5 mL) was added I_2 (158 mg, 0.62 mmol) and methanol (30 mL). The mixture was stirred for 10 min, and then placed in a refrigerator at 4 °C for 24 h. The resulting brown microcrystalline product was collected by filtration, washed with methanol, and dried under vacuum (yield: 470 mg, 83%). Single crystals suitable for X-ray structural analysis were obtained by diffusing diethyl ether into an acetonitrile solution of **1**. Elemental analysis: Calcd for $C_{20}H_9N_5S_4F_3Ni$: C, 42.6; H, 1.60; N, 12.4%. Found: C, 42.8; H, 1.71; N, 12.3%.

$[F_3BzPy][Pd(mnt)_2]$ (2) and $[F_3BzPy][Pt(mnt)_2]$ (3)

The procedure described for **1**, except with the corresponding derivatives of [fluorobenzyl)pyridinium]$_2[M(mnt)_2]$ (M = Pd or Pt) as the starting material, was followed to afford **2** and **3**. Elemental analysis: Calcd for $C_{20}H_9N_5S_4F_3Pd$ (**2**): C, 39.3; H, 1.48; N, 11.5%. Found: C, 39.3; H, 1.76; N, 11.4%. $C_{20}H_9N_5S_4F_3Pt$ (**3**): C, 34.3; H, 1.30; N, 10.0%. Found: C, 34.4; H, 1.32; N, 9.97%.

The preparation of crystal **4** was described previously.[8k]

Magnetic susceptibility

Magnetic susceptibility measurements on polycrystalline samples were carried out with a Quantum Design MPMS-XL superconducting quantum interference device (SQUID) magnetometer between 2–350 K under a magnetic field of 1 T.

Heat capacity

The measurement of C_p for **4** was performed by the relaxation method using a Quantum Design PPMS in the temperature range 2–140 K. A crystal with a mass of 0.52 mg was attached to the sample platform using a small amount of grease.

X-Ray structural analyses

Crystallographic data for **1–3** were collected using a Rigaku RAXIS RAPID diffractometer with Mo Kα (λ = 0.71073 Å) radiation from a graphite monochromator. Structures were solved by direct methods using the SHELXL-97 software package.[11] The non-H atoms were refined anisotropically using the full-matrix least-squares method on F^2. All H atoms were placed at calculated positions (C–H = 0.930 Å for benzene or pyridine rings and 0.970 Å for methylene) and refined riding on the parent atoms with $U(H) = 1.2 \times U\text{eq}$ (bonded C atom). Details of the crystal parameters, data collection, and refinement for **1–3** are summarized in Table 2. The bond lengths in $[M(mnt)_2]^-$ (M = Ni, Pd or Pt) anions, along with their estimated standard deviations, are listed in Table S1 of the ESI.† Some important intermolecular distances are listed in Table 3.

CCDC reference numbers 182194 and 285872–285874.

For crystallographic data in CIF or other electronic format see DOI: 10.1039/b514278d

Temperature dependent oscillation photographs

The oscillation photographs at different temperature for **4** were taken using a Rigaku RAXIS RAPID imaging plate area detector with graphite monochromated Mo Kα radiation (λ = 0.71073 Å).

Results and discussion

Crystal structures of 1, 2 and 3

The complexes **1**, **2** and **3** are isomorphous, so only the detailed structure of **1** is presented here. The asymmetric unit within the unit cell of **1**, comprised of one $[Ni(mnt)_2]^-$ together with one F_3PyBz^+, is shown in Fig. 1(a). The anion possesses a

Table 2 Crystallographic data for **1–4**

Complex	**1**	**2**	**3**	**4**
Mol. formula	$C_{20}H_9F_3N_5NiS_4$	$C_{20}H_9F_3N_5PdS_4$	$C_{20}H_9F_3N_5PtS_4$	$C_{20}H_{11}FN_5NiS_4$
Temp./K	100	293	293	293
CCDC no.	CCDC-285872	CCDC-285873	CCDC-285874	CCDC-182194
Mol. mass	563.27	610.96	699.65	527.29
Space group	$P2_1/c$	$P2_1/c$	$P2_1/c$	$P2_1/c$
a/Å	7.445(2)	7.4749(15)	7.5498(15)	12.112(2)
b/Å	22.234(6)	22.786(5)	22.745(5)	25.875(5)
c/Å	13.400(5)	13.566(3)	13.546(3)	7.3230(15)
α/°	90	90	90	90
β/°	98.400(10)	98.55(3)	98.70(3)	101.72(3)
γ/°	90	90	90	90
V/Å^3	2194.3(12)	2284.8(8)	2299.3(8)	2247.2(7)
Z	4	4	4	4
μ/mm^{-1}	1.310	1.221	6.509	1.261
λ/Å	0.71070	0.71070	0.71070	0.71070
ρ/g cm^{-3}	1.705	1.776	2.021	1.559
R_1[a]	0.0288	0.0525	0.0387	0.0353
wR_2[b]	0.0548	0.1045	0.0838	0.0781

[a] $R_1 = \sum(||F_o| - |F_c||)/\sum|F_o|$. [b] $wR_2 = \sum w(|F_o|^2 - |F_c|^2)^2/\sum w(|F_o|^2)^2]^{1/2}$.

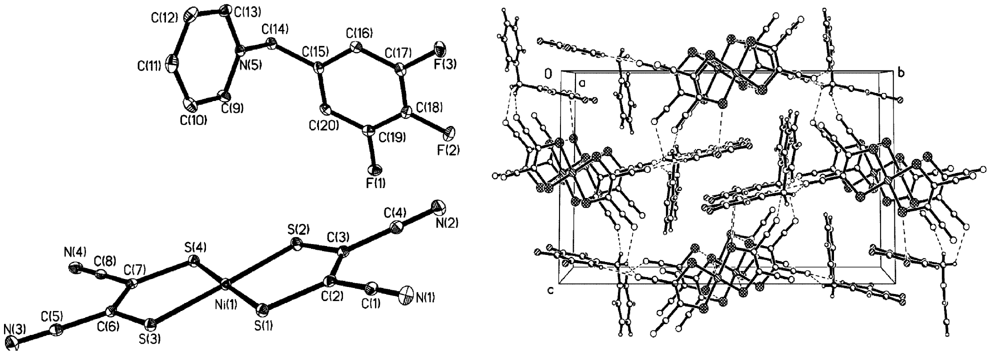

(a) (b)

Fig. 1 (a) ORTEP[11] diagram of **1** (with displacement ellipsoids at a 30% probability level) and H atoms omitted for clarity. (b) Packing diagram of **1** showing the anionic stacks along the direction of *a*-axis.

roughly planar geometry, and most of the bond lengths and angles are in good agreement with various $[Ni(mnt)_2]^-$ complexes.[8] Similar to other members of the [RBzPy][Ni(mnt)$_2$] series, the anions form columnar stacks which lie parallel to the *a*-axis (Fig. 1(b)). Within an anionic stack, two kinds of overlapping patterns between neighbors were observed, as shown in Fig. 2. Face-to-face overlapping (eclipse overlapping) involves an anionic pair containing Ni(1) and Ni(1)^i (symmetry code $i = 1 - x$, $2 - y$, $1 - z$) in which the nearest Ni···Ni distance (3.420 Å) is comparable to the corresponding interplane distance (3.433 Å) (the mean molecular plane is defined by four coordinated S atoms). Longitudinal and transverse offsets involve an anionic pair containing Ni(1) and Ni(1)^{ii} (symmetry code $ii = 2 - x$, $2 - y$, $1 - z$) in which the Ni···Ni and corresponding interplane distances are 4.465 and 3.484 Å, respectively. In other words, the anionic stack is irregular and dimeric which is different from that found in **4**.

In the complexes with substituted benzylpyridinium derivatives, the molecular configuration was completely determined by three dihedral angles, which were the angles between the benzene ring and reference plane (defined by C_{Ar}–CH_2–N_{Py}), between the pyridine ring and reference plane, and between the benzene and pyridine rings. For convenience, these dihedral angles are represented by θ_1, θ_2 and θ_3, respectively, and are summarized in Table 4. In **1**, θ_1, θ_2 and θ_3 are 102.3, 116.3 and 108.2°, respectively. The angles θ_1 and θ_3 are of comparable value within the series, but the value of θ_2 for **4** differs markedly from those measured in **1–3**.[8k] As demonstrated in Fig. 2(c) and (d), the benzene rings between the adjacent cations keep away from each other which is probably due to the steric repulsion between the F atoms (the steric repulsion should become stronger with an increase in the number F atoms on the benzene ring). As a result, the cations in **1–3** do not form the columnar stacks (*cf.* Fig. 1(b)) that are a common feature of the stacking patterns in the series of the benzylpyridinium derivatives with [M(mnt)$_2$] (M = Ni, Pd or Pt).

Magnetic susceptibility

The magnetic behaviors of **1–3** have been determined using polycrystalline samples between 2–350 K. The results are given in Fig. 3 as $\chi_m = f(T)$. As shown in Fig. 3, they all exhibited a very weak paramagnetism. For **2** and **3**, $\chi_m = f(T)$ follows the

Table 3 Intermolecular short separations or interplane distances (in Å) between the nearest-neighboring anions for **1–4**

	1		**2**		**3**		**4**	
Overlap	AB	BA′	AB	BA′	AB	BA′	AB	BA′
M···M	3.420	4.465	3.392	4.493	3.452	4.532	3.937	3.937
M···S	Ni(1)···S(2) 4.013 Ni(1)···S(1) 4.080 Ni(1)···S(4) 4.032 Ni(1)···S(3) 4.058	Ni(1)···S(2) 3.652	Pd(1)···S(2) 4.053 Pd(1)···S(4) 4.091	Pd(1)···S(2) 3.707	Pt(1)···S(2) 4.070 Pt(1)···S(1) 4.154 Pt(1)···S(3) 4.183 Pt(1)···S(4) 4.151	Pt(1)···S(2) 3.750	Ni(1)···S(1) 4.207 Ni(1)···S(2) 3.646	Ni(1)···S(1) 3.598
S···S	S(2)···S(3) 3.406 S(1)···S(4) 3.462	S(2)···S(2) 3.998 S(1)···S(2) 3.739	S(1)···S(4) 3.443 S(2)···S(3) 3.395	S(1)···S(2) 3.864	S(2)···S(3) 3.442 S(1)···S(4) 3.508	S(1)···S(2) 3.880	S(1)···S(3) 3.937 S(2)···S(2) 3.832	S(1)···S(3) 3.832 S(2)···S(2) 3.832 S(3)···S(1) 3.750
Plane-to-plane	3.433	3.484	3.4183	3.5767	3.474	3.608	3.531	3.558
Symmetry operations applied to the second atom for AB or BA′	$1 - x, 2 - y, 1 - z$	$2 - x, 2 - y, 1 - z$	$1 - x, 2 - y, 1 - z$	$2 - x, 2 - y, 1 - z$	$1 - x, 2 - y, 1 - z$	$2 - x, 2 - y, 1 - z$	$x, -0.5 - y, -0.5 + z$	$x, -0.5 - y, 0.5 + z$

Table 4 Dihedral angles (in °) in the cation moieties of complexes **1–4**

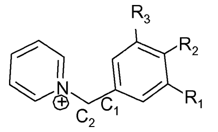

	1	**2**	**3**	**4**
θ_1	102.3	100.6	100.1	103.0
θ_2	116.3	116.2	115.5	98.0
θ_3	108.2	108.4	108.7	112.4

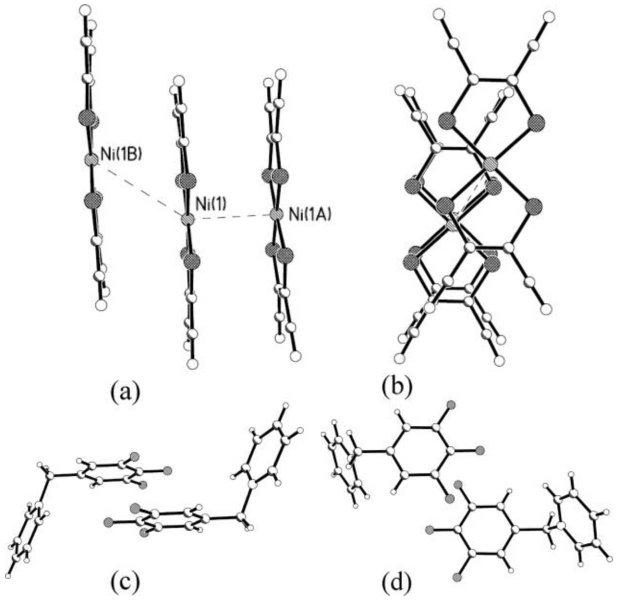

Fig. 2 The anionic arrangement patterns for **1** as viewed from (a) the side and (b) above (symmetry codes: 1A = $-x, -2 - y, 1 - z$; 1B = $1 - x, -2 - y, 1 - z$). The cationic arrays for **1** as viewed from (c) the side and (d) above .

Curie–Weiss law, whereas in the case of **1** the typical magnetic behavior of a spin gap system was observed. Therefore, eqn (1) was used to fit the temperature dependence of the magnetic susceptibilities of **2** and **3**

$$\chi_m = \frac{C}{T - \theta} + \chi_0 \qquad (1)$$

while eqn (2) was used for **1**

$$\chi_m = \frac{\alpha}{T} \exp(-\Delta/T) + \frac{C}{T} + \chi_0 \qquad (2)$$

where α is a constant value corresponding to the dispersion of excitation energy, Δ is the magnitude of the spin gap, χ_0 contributes from the core diamagnetism and the possible Van Vleck paramagnetism.[12] The best fitting yielded the parameters of $\alpha = 6.8(7)$ emu K mol^{-1}, $\Delta/k_B = 2474(23)$ K, $C = 3.6(1) \times 10^{-4}$ emu K mol^{-1}, and $\chi_0 = -2.4(1) \times 10^{-4}$ emu mol^{-1} for **1**; $C = 1.39(1) \times 10^{-3}$ emu K mol^{-1}, $\theta = -0.58(2)$ K and $\chi_0 = -1.7(1) \times 10^{-4}$ emu mol^{-1} for **2**, $C = 3.6(3) \times 10^{-3}$ emu K mol^{-1}, $\theta = -0.49(1)$ K and $\chi_0 = -1.59(2) \times 10^{-4}$ emu mol^{-1} for **3**. The χ_0 values in **1–3** range from -1.6×10^{-4} to -2.4×10^{-4} emu mol^{-1}, which are comparable to their diamagnetic corrections calculated from tabulating Pascal constants. For **1**, the spin gap leads to

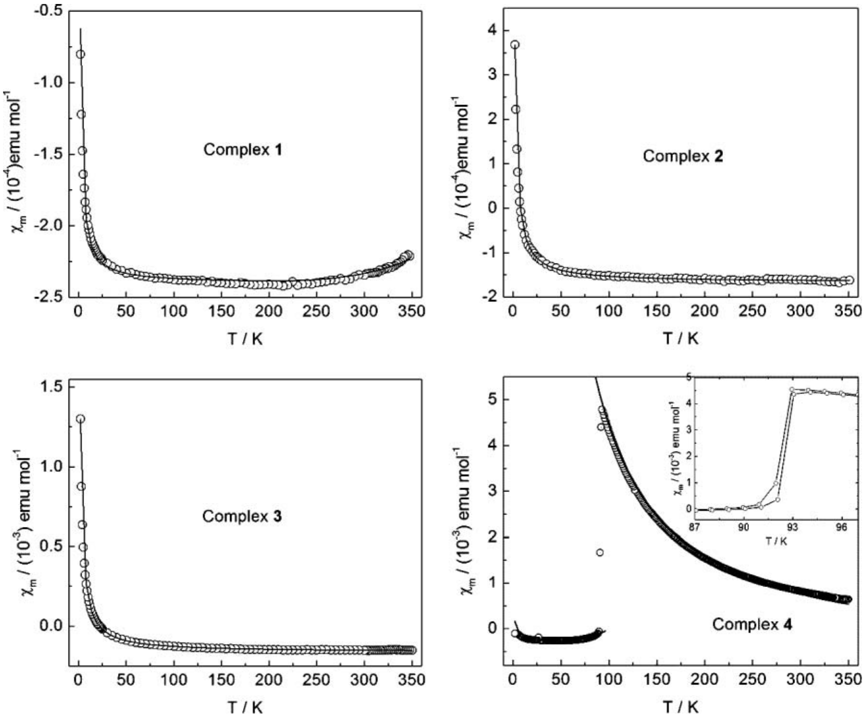

Fig. 3 Temperature dependence of the magnetic susceptibilities of **1–4** (open circles: experimental data; solid lines: fitted data. The inset in the graph of **4** shows the hysteresis loop).

the magnetic susceptibility decreasing exponentially upon cooling at higher temperature region. For **2** and **3**, the very small Curie constant indicated that the weak paramagnetism originates from magnetic impurities, and hence the inherent magnetic behaviors of both **2** and **3** should be diamagnetic due to the existence of very strong antiferromagnetic coupling interactions in the eclipsed $[M(mnt)_2]^-$ (M = Pd or Pt) pair in the anionic stack. The distinction between the magnetic behaviors of $[Ni(mnt)_2]^-$ and $[M(mnt)_2]^-$ (M = Pd or Pt) series (the former possesses a finite energy gap whereas the latter are diamagnetic), indicates that the antiferromagnetic exchange interactions are much stronger in $[M(mnt)_2]^-$ (M = Pd or Pt) than in $[Ni(mnt)_2]^-$, which is associated with the fact that a more efficient molecular orbital overlap takes place in $[M(mnt)_2]^-$ (M = Pd or Pt) complexes due to the bigger ionic radii of Pd and Pt [*cf.* Table 3, the plane-to-plane distances in the eclipsed overlapping pair of anions for **1–3** are comparable to each other].

As is illustrated in Fig. 3, the prominent magnetic characteristics of **4** are a peculiar spin transition that occurs at ~93 K, the ferromagnetic coupling that dominates above this transition (high temperature phase, abbreviated as HT phase) and a spin gap that opens below the transition (low temperature phase, abbreviated as LT phase).

In the HT phase, the Baker equation (eqn (3)),[13] derived from a high temperature series expansion for a ferromagnetic chain, is used to analyze the magnetic susceptibility, and the contribution (χ_0) originating from the closed shells (diamagnetism) and possible Van Vleck paramagnetism was further taken into account (eqn (4))

$$\chi_{\text{chain}} = \frac{Ng^2\mu_B^2}{4k_BT}\left[\frac{C}{D}\right]^{2/3} \qquad (3)$$

$$\chi_m = \chi_{\text{chain}} + \chi_0 \qquad (4)$$

where $C = 1.0 + 5.7979916y + 16.902653y^2 + 29.376885y^3 + 29.832959y^4 + 14.036918y^5$, $D = 1.0 + 2.7979916y + 7.008678y^2 + 8.653644y^3 + 4.5743114y^4$ and $y = J/k_BT$. The best fit for the magnetic susceptibility above 93 K yielded the parameters, $J/k_B = 15.2(3)$ K and $\chi_0 = -3.7(8) \times 10^{-4}$ emu mol^{-1} with a fixed g-factor of 2.035 (which was determined from the room temperature EPR spectrum, see Fig. S6 of the ESI†).

Below the transition, a spin-Peierls-like dimeric lattice distortion[5,8,14,15] happens which is supported by the fact that the XRD pattern is more complicated in the LT than the HT phase,[8k] and several new diffractions were observed in LT phase to indicate the symmetry of the lattice is lowered upon moving from HT to LT phase.[16] Eqn (2) is accordingly used to evaluate the temperature dependence of the magnetic susceptibility. A reasonable fit of the magnetic susceptibility data in the temperature range of 4–88 K gave the parameters $\alpha = 9.04(43)$, $\Delta/k_B = 581(12)$ K, $\chi_0 = -2.8(1) \times 10^{-4}$ emu mol^{-1}, $C = 8.8(6) \times 10^{-4}$ emu K mol^{-1}.

For the magnetic behavior of **4**, our initial questions regarding the origin of the ferromagnetic interaction in the HT phase and the cause of the switch in the nature of the magnetic exchange in the HT and LT phases, are interesting. Coomber *et al.*[4c] calculated the spin density distributions in a single $[Ni(mnt)_2]^-$ anion at the UHF/INDO level, and the results indicated that the Ni ion and S atoms possess large positive and small negative spin densities, respectively. Based on these calculations, they thought that the spin-polarization effect plays an important role in the magnetic exchange process and gave the following physical picture about the nature of magnetic exchange, namely, for the $[Ni(mnt)_2]^-$ neighbors overlapping in a slipped Ni-over-S configuration, the spin polarization effect (McConnell's theory[17]) between large positive spin densities on Ni ions and small negative spin densities on S atoms of adjacent anions of $[Ni(mnt)_2]^-$ leads to a ferromagnetic coupling interaction (illustrated in Fig. 4(a)), while the direct overlapping of Ni$\cdots$Ni or S$\cdots$S gives rise to an antiferromagnetic coupling interaction. In fact, a slipped Ni-over-S stacking pattern was observed in the anionic stack of **4** as depicted in Fig. 4(b). In our most recent study,[18] we recalculated the spin distributions in a dimer of [Ni(mnt)$_2$]$^-$ utilizing a series of functionals and basis sets in the framework of density functional theory (DFT) and found that the calculated spin populations depended upon the method used. Among them, the values of spin density distributions at the UBPW91/LANL2DZ level matched the EPR experimental results well, which revealed that the S atoms possessed large spin densities, but the centre Ni ion did not due to the strong delocalization effect from the Ni ion to mnt^{2-} ligands, and that the sum of the spin population in the core of NiS$_4$ was 0.887 from our calculation *vs* 0.85 from experiment.[19] However, our results do not match the report by Coomber *et al.*[4c] In addition, we examined the variation of the magnetic exchange constant (*J*) in a [Ni(mnt)$_2$]$^-$ dimer as a function of the interplane distance as well as the rotation angle (θ)[18] [the angle made by the long molecular axis of each monomer] by the symmetry-broken method in the DFT framework and the X-ray structures. The results indicated that the nature of the magnetic exchange in a [Ni(mnt)$_2$]$^-$ dimer is sensitive to these two factors, and the switching of the magnetic exchange nature between ferromagnetic and antiferromagnetic is probably achieved by changes in the interplane distance or rotation angle (θ). The magnetic orbital interaction is the main contributor to the spin transition and magnetic exchange characteristics of a spin system even if weak spin-polarization effect exists in the system. Therefore, the peculiar magnetic behavior of **4** can be interpreted as follows. The [Ni(mnt)$_2$]$^-$ array within a stack in the HT phase accidentally satisfy the conditions required for a ferromagnetic interaction, but, upon cooling, the anisotropic contraction of the crystal leads to a non-uniform compression and slippage of the [Ni(mnt)$_2$]$^-$ stack, which trigger the spin transition.

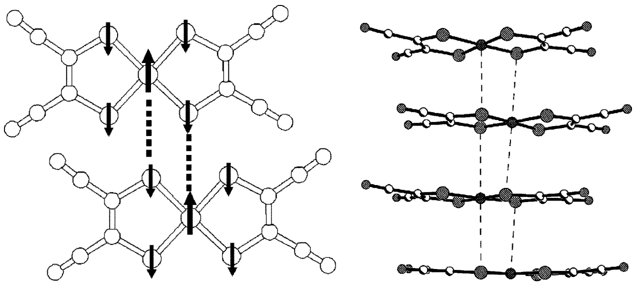

(a) (b)

Fig. 4 (a) Schematic representation of spin density distributions in [Ni-(mnt)$_2$]$^-$. The dotted line shows the 'local' antiferromagnetic interactions. (b) Ni-over-S stacking pattern observed in an anionic stack of **4**.

Heat capacity

Fig. 5 shows the results of the heat capacity measurement for **4**. A sharp thermal abnormality with λ-shape, which is a typical feature of first order transitions, was observed, and the peak temperature, at 93.4 K, coincides fairly well with the temperature where the abrupt drop of susceptibility takes place.

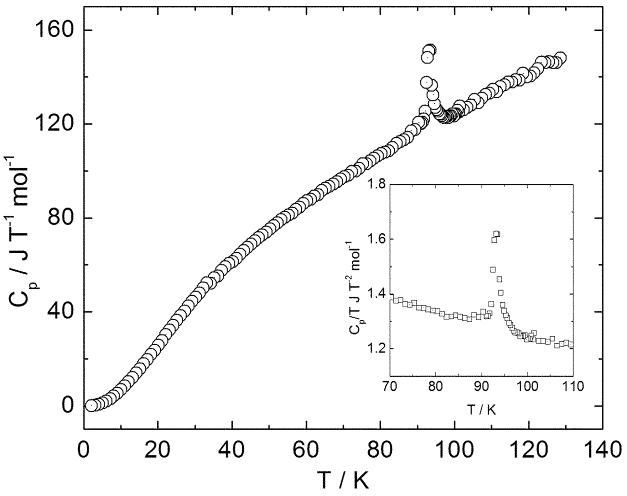

Fig. 5 Temperature dependence of molar heat capacity of crystal **4**, the inset shows the plot of C_p/T *vs* *T*.

In the first order approximation, a normal heat capacity is considered a smooth curve.[20] Upon subtracting this contribution from the normal heat capacity, the entropy change of this transition is estimated as 1.02 J K^{-1} mol^{-1}, and this value is less than the theoretical maximum of spin entropy for a mole of $S = \frac{1}{2}$ ions, $R\ln2 \approx 5.76$ J K^{-1} mol^{-1},[3a] suggesting that the short range order persists over the temperature of the transition in **4**. The short range ordering is an indication of the lowered dimensionality of the magnetic system, and is consistent with the chain structure of [Ni(mnt)$_2$]$^-$ in crystal **4**.[21]

Superlattice diffractions

Local structural fluctuation is a common phenomenon existing in the quasi-one-dimensional conductor or magnet which originates from electron–phonon or magnetoelastic coupling interactions. Fig. 6 displays the temperature dependent diffraction patterns, from which the superlattice diffractions were observed below 140 K and became stronger upon cooling. This observation provided the evidence that the pretransitional structural fluctuation exists above the transition temperature.

Conclusion

The crystal structures and magnetic properties were measured for three new ion-pair complexes which consist of derivatives of multi-fluorine substituted benzylpyridinium with [M(mnt)$_2$]$^-$ (M = Ni, Pd or Pt). The dependence of the stacking effect on the nature of the substituent groups was observed, and the common stacking pattern of the cations seen for the series of [M(mnt)$_2$]$^-$ with mono-substituted benzylpyridinium derivates, in which adjacent benzene rings overlap in a face-to-face fashion, was not seen in **1–3**. Instead, the neighboring cations keep away from each other due to steric and/or electrostatic repulsion between the multi-substituted benzene rings. As a result, the cations do not form columnar stacks in the solid state. The anionic stacking columns dimerize in **1–3**. The complexes [Pd(mnt)$_2$]$^-$ and [Pt(mnt)$_2$]$^-$ are diamagnetic, while the complex [Ni(mnt)$_2$]$^-$ possesses an energy gap of 2274 K. This difference originates from the greater molecular orbital overlap in

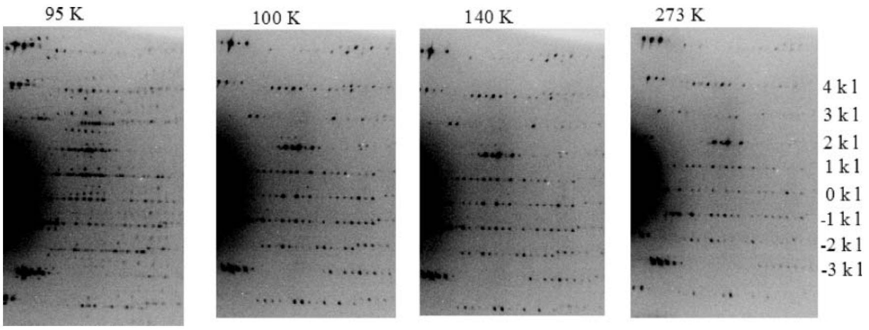

Fig. 6 Temperature dependent oscillation photographs of **4** which show superlattice diffractions below 140 K.

dimers of $[M(mnt)_2]^-$ (M = Pd or Pt) than $[Ni(mnt)_2]^-$ due to the ionic radii of Pd and Pt being much larger than Ni.

The sharp thermal anomaly with λ-shape seen for **4** associated with the spin transition indicated that the transition was of first order and the superlattice diffraction provided evidence for a pretransitional phenomena up to at least 140 K. The theoretical study suggested the magnetic exchange nature in a $[Ni(mnt)_2]^-$ complex depends highly on parameters relating to the stacking pattern, such as the distance between intermolecular planes and the rotation angle between the long molecular axes. Therefore, the anisotropic contraction of the crystal **4** upon cooling led to the non-uniform compression and slippage of the $[Ni(mnt)_2]^-$ stack, which could be responsible for the variation of the nature of the magnetic exchange and triggering the spin transition.

Acknowledgements

This work was partly supported by a Grant-in-Aid for Science Research from the Ministry of Education, Culture, Sports, Science and Technology of Japan. Authors thank Prof. I. Nomura and Dr Ichimura for use of the SQUID magnetometer. Ren (JSPS fellow ID No. P03271) thanks the Japan Society for the Promotion of Science for financial support.

References

1 (*a*) J. L. Brusso, O. P. Clements, R. C. Haddon, M. E. Itkis, A. A. Leitch, R. T. Oakley, R. W. Reed and J. F. Richardson, *J. Am. Chem. Soc.*, 2004, **126**, 8256; (*b*) J. S. Miller, *Angew. Chem., Int. Ed.*, 2003, **42**, 27; (*c*) M. E. Itkis, X. Chi, A. W. Cordes and R. C. Haddon, *Science*, 2002, **296**, 1443.

2 E. Laukhina, J. Vidal-Gancedo, V. Laukhin, J. Veciana, L. Chuev, V. Tkacheva, K. Wurst and C. Rovira, *J. Am. Chem. Soc.*, 2003, **125**, 3948.

3 (*a*) W. Fujita, K. Awaga, Y. Nakazawa, K. Saito and M. Sorai, *Chem. Phys. Lett.*, 2002, **352**, 348; (*b*) W. Fujita and K. Awaga, *Science*, 1999, **286**, 261; (*c*) H. Nishikawa, A. Machida, T. Morimoto, K. Kikuchi, T. Kodama, I. Ikemoto, J. Yamada, H. Yoshino and K. Murata, *Chem. Commun.*, 2003, 494.

4 (*a*) T. Nakamura, T. Akutagawa, K. Honda, A. E. Underhill, A. T. Coomber and R. H. Friend, *Nature*, 1998, **394**, 159; (*b*) A. E. Pullen, C. Faulmann, K. I. Pokhodnya, P. Cassoux and M. Tokumoto, *Inorg. Chem.*, 1998, **37**, 6714; (*c*) A. T. Coomber, D. Beljonne, R. H. Friend, J. L. Brédas, A. Charlton, N. Robertson, A. E. Underhill, M. Kurmoo and P. Day, *Nature*, 1996, **380**, 144; (*d*) I. D. Parker, R. H. Friend, P. I. Clemenson and A. E. Underhill, *Nature*, 1986, **324**, 547.

5 J. Nishijo, E. Ogura, J. Yamaura, A. Miyazaki, T. Enoki, T. Takano, Y. Kuwatani and M. Iyoda, *Solid State Commun.*, 2000, **116**, 661.

6 (*a*) S. B. Bulgarevich, D. V. Bren, D. Y. Movshovic, P. Finocchiaro and S. Failla, *J. Mol. Struct.*, 1994, **317**, 147; (*b*) G. Montaudo, S. Caccamese and P. Finocchiaro, *J. Am. Chem. Soc.*, 1971, **93**, 4202.

7 (*a*) X. M. Ren, T. Akutagawa, S. Nishihara and T. Nakamura, *Synth. Met.*, 2005, **150**, 57; (*b*) J. L. Xie, X. M. Ren, Y. Song, Y. Zou and Q. J. Meng, *J. Chem. Soc., Dalton Trans.*, 2002, 2868.

8 (*a*) X. M. Ren, T. Akutagawa, S. Nishihara, T. Nakamura, W. Fujita and K. Awaga, *J. Phys. Chem. B*, 2005, **109**, 16610; (*b*) C. L. Ni, D. B. Dang, Y. Z. Li, S. Gao, Z. P. Ni, Z. F. Tian and Q. J. Meng, *J. Solid State Chem.*, 2005, **178**, 100; (*c*) C. L. Ni, Y. Z. Li, D. B. Dang, Z. P. Ni, Z. F. Tian, Z. R. Yuan and Q. J. Meng, *Inorg. Chem. Commun.*, 2005, **8**, 105; (*d*) D. B. Dang, C. L. Ni, Y. Bai, Z. F. Tian, Z. P. Ni, L. L. Wen, Q. J. Meng and S. Gao, *Chem. Lett.*, 2005, **34**, 680; (*e*) X. M. Ren, H. Okudera, R. K. Kremer, Y. Song, C. He, Q. J. Meng and P. H. Wu, *Inorg. Chem.*, 2004, **43**, 2569; (*f*) C. L. Ni, D. B. Dang, Y. Song, S. Gao, Y. Z. Li, Z. P. Ni, Z. F. Tian, L. L. Wen and Q. J. Meng, *Chem. Phys. Lett.*, 2004, **396**, 353; (*g*) C. L. Ni, D. B. Dang, Y. Z. Li, Z. R. Yuan, Z. P. Ni, Z. F. Tian and Q. J. Meng, *Inorg. Chem. Commun.*, 2004, **7**, 1034; (*h*) J. L. Xie, X. M. Ren, C. He, Z. M. Gao, Y. Song, Q. J. Meng and R. K. Kremer, *Chem. Phys. Lett.*, 2003, **369**, 41; (*i*) X. M. Ren, Q. J. Meng, Y. Song, C. S. Lu, C. J. Hu and X. Y. Chen, *Inorg. Chem.*, 2002, **41**, 5686; (*j*) X. M. Ren, Q. J. Meng, Y. Song, C. J. Hu, C. S. Lu, X. Y. Chen and Z. L. Xue, *Inorg. Chem.*, 2002, **41**, 5931; (*k*) J. L. Xie, X. M. Ren, Y. Song, W. W. Zhang, W. L. Liu, C. He and Q. J. Meng, *Chem. Commun.*, 2002, 2346.

9 X. M. Ren, J. L. Xie and Q. J. Meng, *Acta Cryatallogr., Sect. E*, 2003, **59**, m855.

10 A. Davison and H. R. Holm, *Inorg. Synth.*, 1967, **10**, 8.

11 G. M. Sheldrick, *SHELXL-97, Program for the Refinement of Crystal Structure*, University of Göttingen, Germany, 1997.

12 L. C. Isett, D. M. Rosso and G. L. Bottger, *Phys. Rev. B*, 1980, **22**, 4739.

13 (*a*) G. A. Baker, G. S. Rushbrooke and H. E. Gilbert, *Phys. Rev. Sect. A*, 1964, **135**, 1272; (*b*) L. Deakin, A. M. Arif and J. S. Miller, *Inorg. Chem.*, 1999, **38**, 5072.

14 T. Hasegawa, R. Kondo, S. Kagoshima, Y. Iwasa, T. Mochida, T. Akutagawa and T. Nakamura, *Synth. Met.*, 2001, **120**, 991.

15 J. P. Cornelissen, J. H. van Diemen, L. R. Groeneveld, J. G. Haasnoot, A. L. Spek and J. Reedijk, *Inorg. Chem.*, 1992, **31**, 198.

16 Actually, the single crystal structural data in the low temperature phase is very helpful for understanding the transition and magnetic behaviors in **4**. Unfortunately, such a transition temperature is near the ultimate temperature, ~90 K, attainable by our cryostat. As a result, we can not obtain the single crystal structural information, and we are seeking a collaboration with other groups.

17 H. M. McConnell, *J. Chem. Phys.*, 1963, **39**, 1910.

18 Z. P. Ni, X. M. Ren, J. Ma, Z. D. Chen, J. L. Xie, C. L. Ni and Q. J. Meng, *J. Am. Chem. Soc.*, 2005, **127**, 14330.

19 (*a*) A. H. Maki, N. Edelstein, A. Davison and R. H. Holm, *J. Am. Chem. Soc.*, 1964, **86**, 4580; (*b*) R. D. H. M. A. Schmitt, *J. Am. Chem. Soc.*, 1968, **90**, 2288; (*c*) J. E. Huyett, S. B. Choudhury, D. M. Eichhorn, P.A. Bryngelson, M. J. Maroney and B. M. Hoffman, *Inorg. Chem.*, 1998, **37**, 1361.

20 K. Saito, M. Massalska-Arodz, S. Ikeuchi, M. Maekawa, J. Sciesinski, E. Sciesinska, J. Mayer, T. Wasiutynski and M. Sorai, *J. Phys. Chem. B*, 2004, **108**, 5785.

21 S. N. Bhatia, C. J. O'Connor, R. L. Carlin, H. A. Algra and L. J. De Jongh, *Chem. Phys. Lett.*, 1977, **50**, 353.